Long Short-Term Memory Neural Networks for Flow Regime Identification using ECT

Rafael Johansen[1], Torbjørn Grande Østby[1], Antoine Dupré[2], Saba Mylvaganam[1*]

[1]Department of Electrical Engineering, IT and Cybernetics, Faculty of Technology, Natural Sciences and Maritime Sciences, University of South-Eastern Norway, 3901 Porsgrunn, Norway
[2]Private Practice, Jouquetti, 05400 Furmeyer, France

*Email: saba.mylvaganam@usn.no

ABSTRACT

In multiphase flow related experiments and simulations, flow regime identification (FRI) and the transitions from one flow regime to the other are of interest to process engineers as well as researchers dealing with computational fluid dynamics (CFD). This paper presents some results using deep learning analytics in identifying flow regimes in water-air flow measurements, using an Electrical Capacitance Tomographic (ECT) system. The ECT system consists of single plane 12-electrodes, operating at 500 fps delivering 66 independent capacitance values in 2 ms. By carefully selecting the corresponding mass flow rates of each phase, an experimental matrix is formed showing the different flow regimes in the flow rig. All measurement series from experiment #1 to #84 were divided into two data groups, training data with 7500 frames and validation data with 7499 frames. All 84 experiments were repeated forming a set of data for testing, whereas the former set was used for training and validation. Pre-processing the data from the experiments referred to in Table 1 was necessary to achieve the right balance of flow regimes before using them in the machine learning algorithms. As the algorithms used in ANN use gradients, which in a typical recurrent neural network (RNN) with many hidden layers can vanish or escalate, the usage of Long Short-Term Memory (LSTM) neural networks circumvent to a certain extent, problems associated with such gradient excursions, at the same retaining memory over short durations. After introducing the neural network architecture consisting of 2 LSTM in hidden layers and the 66 capacitance values as inputs delivering 5 outputs for the annular, plug, slug, stratified and wavy flow regimes, the success scenario of the algorithm in FRI of the five regimes are presented. The presented results show that the LSTM network is successful in FRI. Some of the wrong FRI results due to anomalies and ambiguities observed in the FRI algorithms can be filtered out by fusing other FRI methods such as the one based on eigenvalues.

Keywords ECT, flow regime identification (FRI), long short-term memory (LSTM), neural networks (NN), machine learning, deep learning.

Industrial Application Oil & Gas, Multiphase flow studies, CFD.

1 INTRODUCTION

There is a growing interest in the process industries to have the machine learning algorithms in their portfolio of process analytics and in their model predictive control. EQUINOR (former STATOIL) has a dedicated group working with machine learning techniques. With big data from a plethora of sensors in the process industries, machine learning based algorithms can support the process engineer in making crucial decisions, particularly with respect to safe and reliable operation of diverse processes.

Multiphase flows occur in many industrial processes and under some circumstances involving particular combinations of different phase fractions and their flow velocities, they can lead to hazards leading to loss of property and lives. These hazardous events in multiphase flows are very often linked to the different flow regimes. In particular, slug flow regime is associated with rapid momentum-flux variations at fittings such as bends (Zhao, 2017).

In the development of CFD algorithms, tuning of different parameters characterizing the fluid dynamic behavior is an essential part. Flow regimes and transitions from one regime to the other are important

in CFD simulations. Experimental data with some indications of the flow regimes within the pipeline can be useful in CFD.

This paper looks into the possibilities of detecting flow regimes and the transition zones between some of them non-invasively using ECT. In the context of flow regime identification and assessment of process parameters, artificial neural networks have been applied successfully in earlier works using regression and prediction techniques using static multiphase studies in stationary pipe sections (Mohamad-Saleh, 2002). This study investigates the possibilities using advanced neural network structures in the timely identification of flow regimes in pilot scale multiphase flow experiments involving at times some intricate transitions between flow regimes. A good introduction to artificial neural networks is given in (Bishop, 1995).

1.1 Machine Learning as an inferential method

Multiphase flows in closed conduits can be studied non-invasively using ECT. In the case of two-phase flows involving air and water, a good representation of the different flow regimes and their transition zones has been presented in (Mandhane et al, 1974). The flow regimes and the corresponding air and water flow rates are shown in Figure 1.

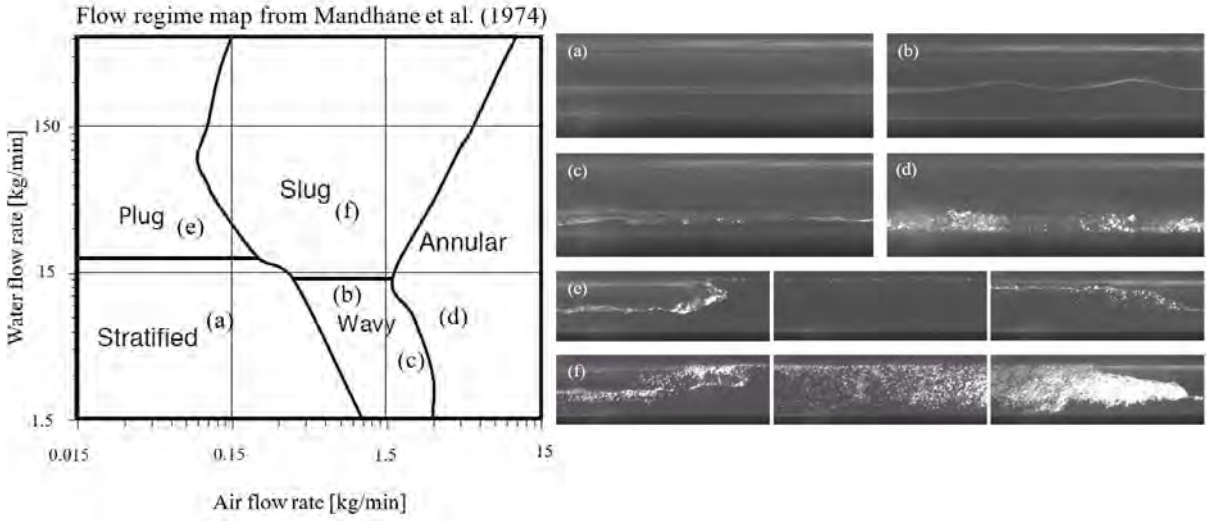

Figure 1. Multiphase flow regimes in two-phase flow involving air and water with actual images form flow studies using 15 m long test section of 56 mm inner diameter. Mass flowrates shown in classification chart, adapted from (Mandhane et al 1974) for flow regimes are from Coriolis meters shown in Figure 3. High-speed video-based images through transparent windows in the test section show (a) stratified, (b) low frequency wavy, (c) high frequency wavy, (d) annular, (e) end, middle and start of a plug and (f) end, middle and start of a slug.

In the context of the present study, the main idea is to use dedicated measurands, viz. electrical capacitance values from an array of electrodes, to classify the flow regimes into five classes, viz. stratified, wavy, plug, slug and annular, as shown in Figure 2.

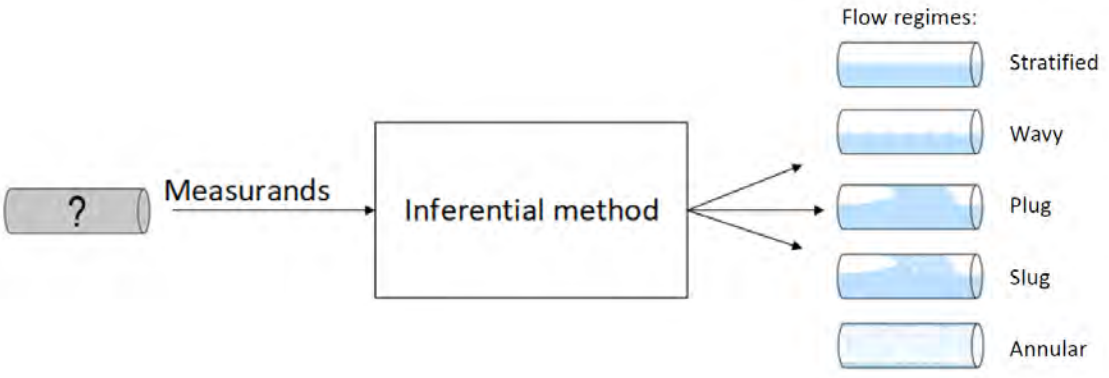

Figure 2. Schematic of inferential method using different measurands; in this study electrical capacitance values using ECT.

2 EXPERIMENTAL SET-UP WITH SENSOR DATA SAMPLING

The details of the multiphase flow rig used in the current study are shown in Figure 3. The flow rig has about 50 measurement points, although in this study, the focus is on the ECT system and the high-speed video images.

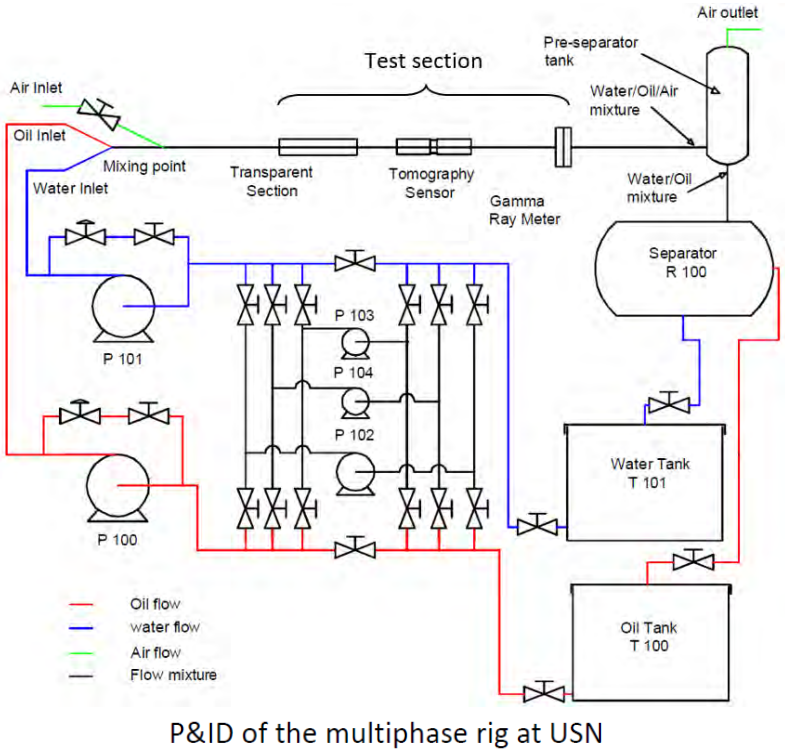

Figure 3. Multiphase flow rig with the 15 m long test section showing the transparent window for high-speed imaging and ECT module. Many other sensors are also used in the tests, (from Pradeep et al, 2012).

2.1 Experimental matrix with different combinations of flow velocities of the two phases.

Using different combinations of air and water flow velocities, 84 experiments were conducted to get the different flow regimes. The various flow velocities of air and water in kg/min as recorded by the Coriolis flowmeter shown in Figure 3 are given in Table 1. The color coding indicates the different observed flow regimes.

Table 1. Matrix with details of 84 two-phase flow experiments for the different flow velocities and volume fractions of water and air. FRI via dedicated transparent observation window in the pipeline. The numbers represent the different experimental runs with the corresponding FRI shown using the color code.

Water [kg/min] \ Air	0.10	0.16	0.25	0.40	0.63	1.00	1.58	2.51	3.98	5.01
79.43	#1	#2	#3	#4						
63.10	#5	#6	#7	#8	#9	#10				
39.81	#11	#12	#13	#14	#15	#16	#17			
25.12	#18	#19	#20	#21	#22	#23	#24	#25		
15.85	#26	#27	#28	#29	#30	#31	#32	#33	#34	
10.00	#35	#36	#37	#38	#39	#40	#41	#42	#43	#44
6.31	#45	#46	#47	#48	#49	#50	#51	#52	#53	#54
3.98	#55	#56	#57	#58	#59	#60	#61	#62	#63	#64
2.51	#65	#66	#67	#68	#69	#70	#71	#72	#73	#74
1.58	#75	#76	#77	#78	#79	#80	#81	#82	#83	#84

Stratified
Slug
Plug
Wavy
Annular

2.2 Sensors and sensor data sampling

The ECT system used in this study has the specifications shown in Table 2.

Table 2. Relevant information about the ECT system used in the two-phase flow experiments using the system shown in Figure 3.

Some specifications for the TFLR5000 ECT-system		Used
Max number of measurement channels	16 (for single-plane)	12
Excitation signal	1-10 MHz	10 MHz
Measurement range	0-2000 fF (femto-Farads)	-
Max data rate	2500 fps (for 16 electrodes)	500

The essential details of selected sensors with focus on sampling rates are given in Table 3. As shown in Table 3, the ECT system delivers 15000 frames of 66 capacitance values in a period of 30s. For this study, the capacitance values from a single plane are used.

Table 3. Duration of sensor data logging with the sampling rates for the sensors used in Figure 3. Each of the 84 experiments in Table 1 contain the amount of data presented in this table.

Duration	Unit	Sample rate	Extra
30 seconds	ECT system	500 fps	15000 frames of 66 capacitances
10 seconds	High Speed Camera	190 fps	1280x480 pixels
60 seconds	Multimodal sensor-suite	20- and 2- fps	500

3 LONG SHORT-TERM MEMORY NETWORK FOR ANALYSING RAW CAPACITANCE VALUES

3.1 Brief introduction to LSTM

Generally, any information has to go through sensory and short-term memory before getting stored in long-term memory. When the content of the long-term memory cannot be retrieved, the phenomenon is called “forgetting”. In the context of machine learning and implementing algorithms, these concepts can be made use of advantageously, depending on the duration and frequency of events under focus.

Slugs and plugs tend to be at low frequencies and the ECT data were obtained at 500 fps as shown in Table 3. In using neural network as a means for machine learning, the events over extended number of time steps need to be in the memory of the network. Hence, LSTM is selected in this study to enable ML. LSTM has some similarities to simple recurrent networks with an internal memory, the contents of which can be accessed by input, output and forget gates, as shown in Figure 4. These gates decide, based on input from the current and the previous time step, whether the unit can be written to, whether it forgets its state, and whether it passes on its current state.

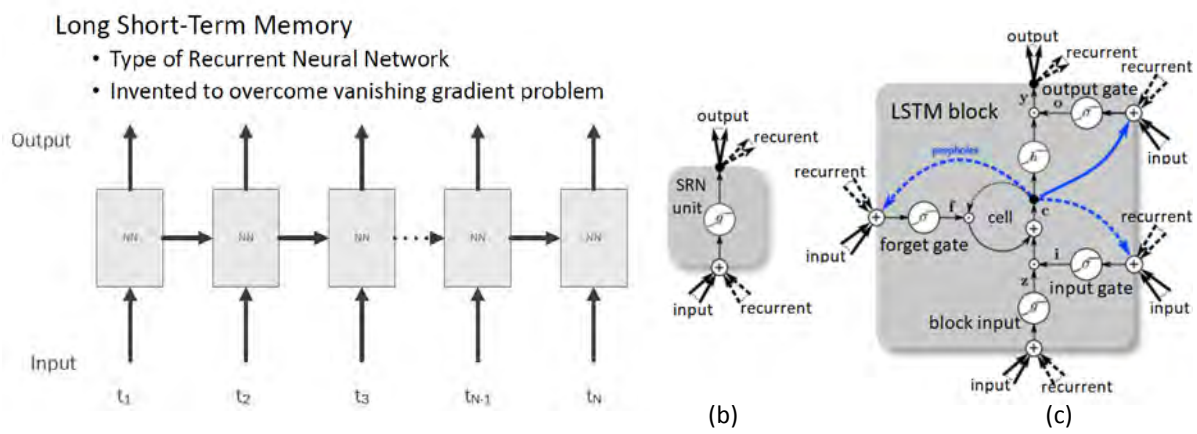

Figure 4. (a) LSTM Schematic representation with input and output across consecutive time instances. (b) While a standard Simple Recurrent Network (SRN) unit only contains one activation function with corresponding input and output, (c) the LSTM block includes additional input, output and forget gates. Figure (b) and (c) (from Deeplearning4J, 2017).

The LSTM network used with ECT raw data, was implemented in Python, using the TensorFlow library (TensorFlow, 2017) and Keras API (KERAS, 2017). The LSTM used here consists of two hidden layers with LSTM units, each with 33 units. The output consisted of 5 fully connected neurons, one for each flow regime class, using “softmax” as activation function. A schematic of the LSTM network used in the current application with the relevant inputs and outputs is given in Figure 5. Some recent developments in the usage of LSTM are described in (Ergen and Kozat, 2017). Algorithmic issues related to LSTM are addressed in (Tilk and Pham, 2017).

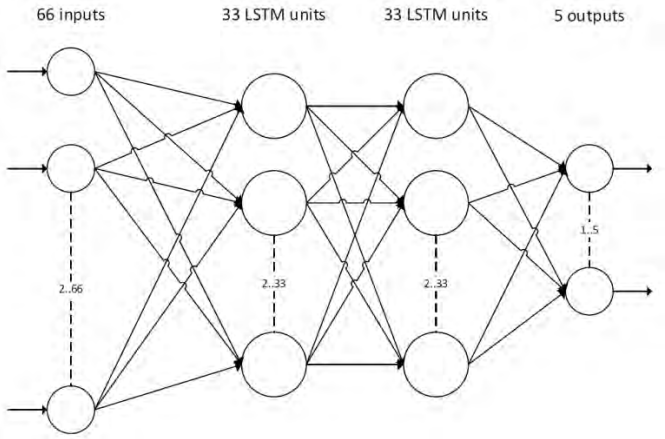

Figure 5. NN Architecture used with validation data using 2 LSTM in hidden layers; 66 capacitance values as inputs; 5 FRI outputs representing annular, plug, slug, stratified and wavy flow regimes.

3.2 Preparation of Experimental Data for Analysis

Each measurement series from experiment #1 to #84 presented in Table 1, was split into two parts, providing one dataset for training, consisting of the first 7500 frames of each experiment, and one for validation, consisting of the remaining 7499 frames. The arrays of capacitance values were concatenated and formatted as row vectors, and 5 columns, one for each flow regime, were inserted at the end of the vector. The column order was the same as in the legend in Table 1. These five columns were filled with ones and zeros according to the observed regimes.

Additionally, datasets similar to the mentioned datasets were created, where the number of samples for each regime type were better balanced. The balance was achieved by oversampling the measurement series classified as plug by a factor of 3, and by under sampling the series classified as stratified by removing some measurement series. The experiments classified as two different flow regimes were discarded in these balanced datasets. Experiment #19 in Table 1, was excluded from the mentioned datasets, as it seemed to be a combination of two shorter measurement series.

Later, all the 84 experiments were retaken to provide a separate dataset for testing.

3.3 Some results from identification of flow regimes using LSTM

Figure 6 (a) – (e) show the FRI outputs as identified by the LSTM network. Results for each of the five flow regimes are shown using the validation sets, and correspond to the visual observations during the experiments. The validation set is a single array compiling 630000 ECT frame data, corresponding to the 84 experiments (with 7500 frames per experiment). The 5 outputs of the model are shown. The final flow regime identification decision is made with the softmax layer. The target is also indicated. An overall good agreement is observed. The LSTM model based FRI has been performed for all experiments except experiment #19.

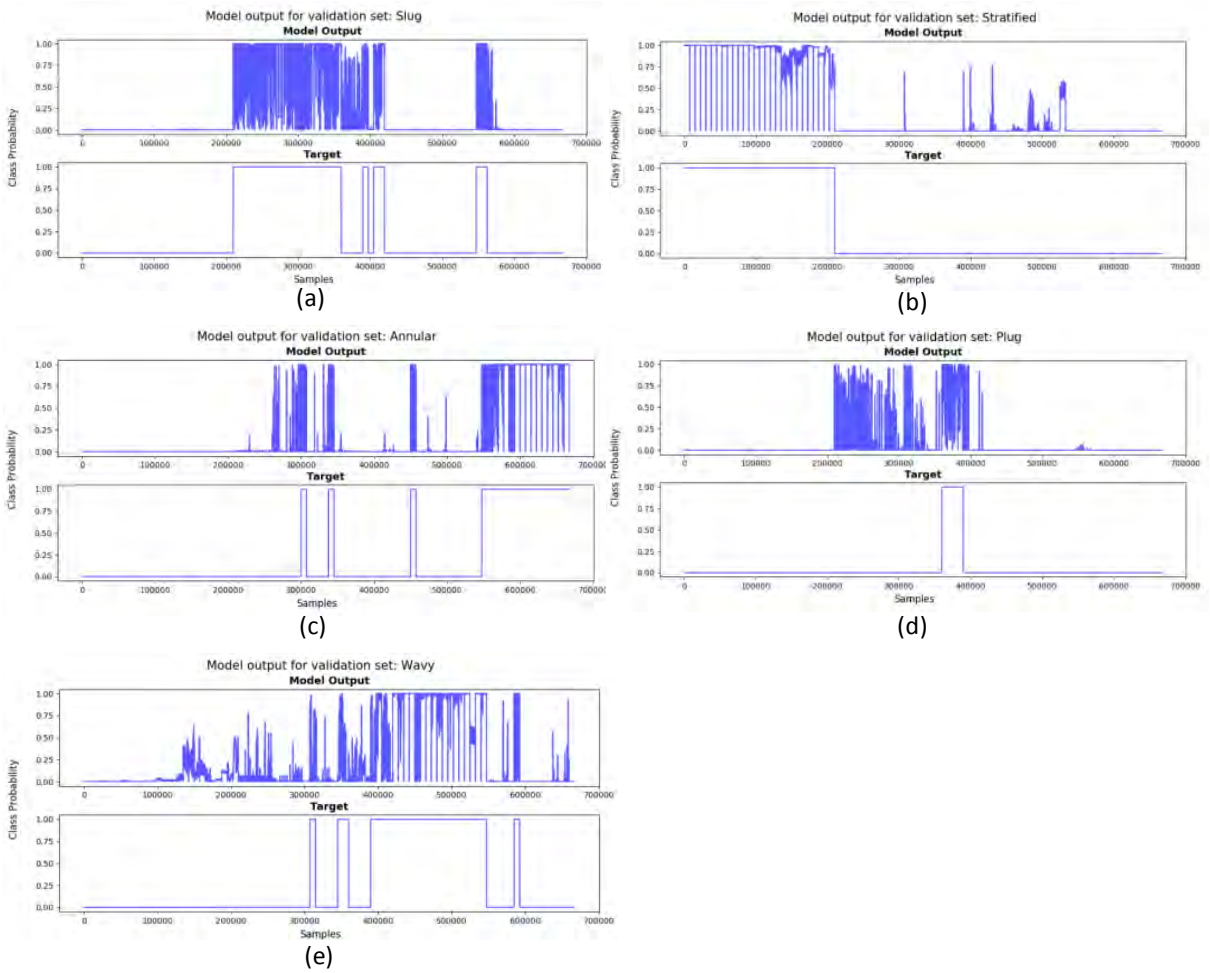

Figure 6. Output and target with respect to the time series for experiment #1 through #84 (excluding #19). Showing the overall model performance for (a) slug, (b) stratified, (c) annular, (d) plug and (e) wavy FRI respectively.

The LSTM network shows for most of the experiments the correct probability class in FRI. The results from the 84 experimental runs with the classifications shown in Table 1, are given in Figure 6. Figure 6 (a) and (d) show some ambiguous moments in the FRI of slugs and plugs, which are somewhat difficult to differentiate even using visual observations and video clips. Figure 6 is based on the measurement dataset used in validation. The results shown in Figure 7 are from a new dataset selected for testing the algorithms. Figure (a) - (e) present model output for single time series representing one typical experiment from each of the five flow regimes.

4 CONCLUSIONS

Using the ECT raw data from 83 experiments, LSTM network was able to classify the flow regimes correctly most of the time. Using LSTM with the validation dataset, an accuracy of more than 96% was achieved in identifying the flow regimes. The accuracy was calculated dividing the number of correctly classified frames by the total number of frames across all experiments. In identifying the transition zones from one type of flow regime to the other, LSTM network performed somewhat less accurate, though correctly identifying some transitions. Transition zones need to be clearly defined using dedicated parameters for machine learning to be successful in identifying them correctly. FRI in the case of slug, plug and annular flows can lead to some ambiguous results, not exclusively because of the malfunctioning of the algorithms, but because of the closely related parameters determining these three phenomena. Fusion of data from the current technique with results based on the techniques using dominant eigenvalues of capacitance matrices as described in (Fang and Cumberbatch, 2015) and (Dupre et al, 2017) can enhance the performance of ECT based FRI. Fusion algorithms including other sensor modalities will also enhance the performance of FRI.

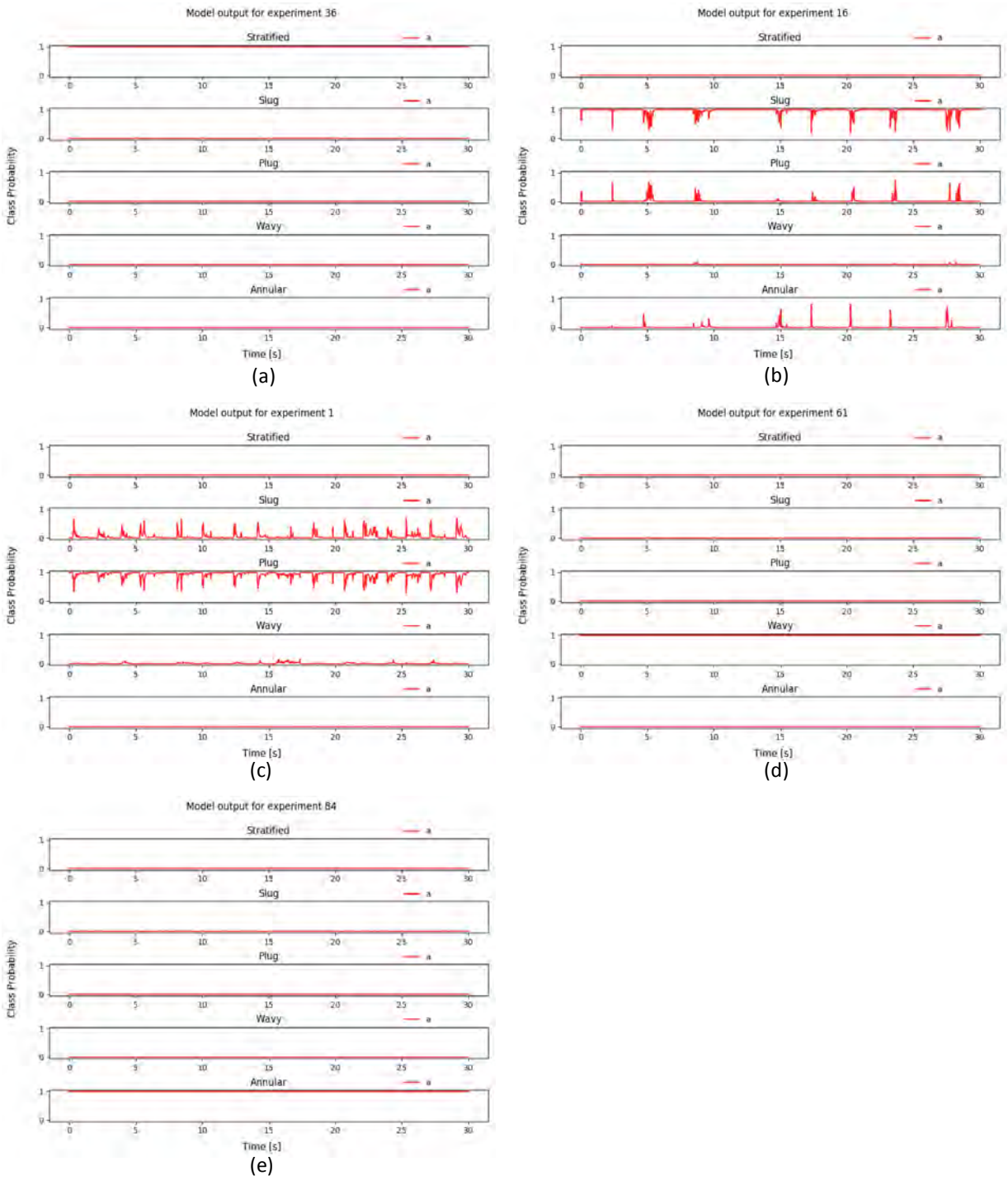

Figure 7. Model output for one experiment from each flow regime corresponding to Table 1. Anomalies/ambiguities possibly due to varying flow regimes in intermittent periods. (a) For experiment #36, correct FRI as stratified. (b) For experiment #16 correctly identified most of the time as slug; at certain intervals identified as plugs. (c) For experiment #1 correctly identified most of the time plug; at certain intervals identified as slugs. (d) For experiment #61, correct FRI most of the time as wavy. (e) For experiment #84, correct FRI most of the time as annular.

5 ACKNOWLEDGEMENT

Mr. Eivind Fjelldalen of USN has been responsible for the hardware involved in the data logging from the sensors used in monitoring the multiphase loop. Docent Dr. Finn Aakre Haugen of USN is responsible for the LabVIEW program used in steering the actuators involved and monitoring various measurements in the multiphase flow rig. Many thanks to Fredrik Hansen of USN for his invaluable help with the operation of the multiphase flow rig and data logging. We acknowledge the assistance of EQUINOR with the multiphase rig, various sensors and the ECT system used in this study.

REFERENCES

BISHOP, C.M. (1995). Neural networks for pattern recognition (Oxford : New York: Clarendon Press ; Oxford University Press).

Deeplearning4J, “A Beginner’s Guide to Recurrent Networks and LSTMs,” [Online]. Available: https://deeplearning4j.org/lstm.html. [Accessed 10.11. 2017].

DUPRE, A., RICCIARDI, G., BOURENANNE, S., and MYLVAGANAM, S. (2017). Electrical Capacitance-Based Flow Regimes Identification—Multiphase Experiments and Sensor Modeling. IEEE Sensors Journal *17*, 8117–8128.

ERGEN, T., and KOZAT, S.S. (2017). Efficient Online Learning Algorithms Based on LSTM Neural Networks. IEEE Transactions on Neural Networks and Learning Systems 1–12.

FANG, W., and CUMBERBATCH, E. (2005). Matrix properties of data from electrical capacitance tomography. Journal of Engineering Mathematics *51*, 127–146.

KERAS, “Keras Documentation,” [Online]. Available: https://keras.io/. [Accessed 10.11. 2017].

MANDHANE, J.M., GREGORY, G.A., and AZIZ, K. (1974). A flow pattern map for gas—liquid flow in horizontal pipes. International Journal of Multiphase Flow *1*, 537–553.

MOHAMAD-SALEH, J., and HOYLE, B.S. (2002). Determination of multi-component flow process parameters based on electrical capacitance tomography data using artificial neural networks. Measurement Science and Technology *13*, 1815–1821.

PRADEEP, C., RU, Y., and MYLVAGANAM, S. (2012). Neural Network-Based Interface Level Measurement in Pipes Using Peripherally Distributed Set of Electrodes Sensed Symmetrically and Asymmetrically. IEEE Transactions on Instrumentation and Measurement *61*, 2362–2373.

TensorFlow, (Online). Available: https://www.tensorflow.org/. [Accessed 10.11.2017].

TILK, O. and PHAM, H., “How does LSTM help prevent the vanishing (and exploding) gradient problem in a recurrent neural network?”, 08.07.2015. [Online]. Available: https://www.quora.com/How-does-LSTM-help-prevent-the-vanishing-and-explodinggradient-problem-in-a-recurrent-neural-network. [Accessed 12.11.2017].

ZHAO, D., OMAR, R., ABDULKADIR, M., ABDULKAREEM, L.A., AZZI, A., SAIDJ, F., HERNANDEZ P., V., HEWAKANDAMBY, B.N., and AZZOPARDI, B.J. (2017). The control and maintenance of desired flow patterns in bends of different orientations. Flow Measurement and Instrumentation *53*, 230–242.